AIP | Applied Physics Letters

Oxygen-induced bi-modal failure phenomenon in SiOx-based resistive switching memory

Yao-Feng Chang, Li Ji, Zhuo-Jie Wu, Fei Zhou, Yanzhen Wang et al.

Citation: Appl. Phys. Lett. **103**, 033521 (2013); doi: 10.1063/1.4816162
View online: http://dx.doi.org/10.1063/1.4816162
View Table of Contents: http://apl.aip.org/resource/1/APPLAB/v103/i3
Published by the AIP Publishing LLC.

Oxygen-induced bi-modal failure phenomenon in SiO_x-based resistive switching memory

Yao-Feng Chang,[1,a)] Li Ji,[1] Zhuo-Jie Wu,[1] Fei Zhou,[1] Yanzhen Wang,[1] Fei Xue,[1] Burt Fowler,[2] Edward T. Yu,[1] Paul S. Ho,[1] and Jack C. Lee[1]
[1]*Department of Electrical and Computer Engineering, Microelectronics Research Center, The University of Texas at Austin, Austin, Texas 78758, USA*
[2]*PrivaTran, LLC, 1250 Capital of Texas Highway South, Bldg 3, Ste 400, Austin, Texas 78746, USA*

(Received 23 May 2013; accepted 3 July 2013; published online 18 July 2013)

The ambient gas effect in SiO_x-based resistive switching memory has been studied. After the electroforming process, resistive switching behavior functions in vacuum as well as in nitrogen without dramatic degradation. However, introducing an oxygen-nitrogen ambient suppresses resistive switching behavior at pressures above 1 Torr. Resistive switching is fully reestablished in oxygen-exposed devices after a vacuum recovery step. The failure phenomena can be described by Monte Carlo simulation using bi-modal statistics to enable feature distribution modeling of failure modes. Design criteria and guidelines are identified for packaging of future oxygen-sensor and of nonvolatile memory applications. © *2013 AIP Publishing LLC*. [http://dx.doi.org/10.1063/1.4816162]

Resistance random access memory (ReRAM) has become a promising candidate for next generation nonvolatile memory due to its potential scalability beyond 10 nm in a cross-bar structure,[1] sub-ns switching speed,[2] sub-pJ energy consumption,[3] low cost, and robust reliability.[4] A simple process with conventional CMOS fabrication, precise control over stack composition, high electrical stability, and good yield are the critical requirements for commercial ReRAM products. Silicon oxide (SiO_x) has been used as gate dielectrics for metal-oxide-semiconductor field effect transistors. In addition to its excellent insulating properties, SiO_x-based resistive switching phenomena have recently been demonstrated in vacuum and atmosphere ambient.[5–7] Although several resistive switching mechanisms have been reported for SiO_x–based devices,[5–7] the exact switching mechanisms are still not well understood due to its unique electrical characteristics where resistive switching behavior only occurs in non-oxidizing ambient and exhibits unique unipolar operation with turn-off voltage being larger in magnitude than turn-on voltage.[8] In this work, the sensitivity to oxygen in SiO_x-based ReRAM has been investigated by controlling the ambient gas pressure and monitoring resistive switching characteristics. Operating stability measurements in vacuum, nitrogen, and oxygen-nitrogen ambients show that SiO_x-based ReRAM is sensitive to oxygen partial pressure, where resistive switching is temporarily disabled. A subsequent vacuum recovery process restores normal functionality. The statistical distribution of electrical parameters in the oxygen-induced device failures can be described using bi-modal Monte Carlo simulations and additional failure analysis. Potential solutions for a unique resistive-switching-type oxygen sensor and packaging methods for SiO_x-based ReRAM are described for development of clear design criteria for future applications.

The SiO_x-based devices were fabricated on n^{++} (100) Si ($1–7 \times 10^{19}\,cm^{-3}$) substrate as bottom electrode with resistivity of 0.001–0.005 Ω-cm.[8] Surface native oxide was removed by 1% dilute HF. A 60 nm-thick SiO_x layer was deposited by magnetron sputtering of silicon target in Ar and O_2 ambient at 200 °C, followed by 5 min post-deposition anneal (PDA) at 500 °C in 1 atm O_2. The top electrode, 200 nm-thick TaN, was sputtered onto the SiO_x film and patterned using reactive ion etching with typically device area being $100 \times 100\ \mu m^2$. CF_4-based plasma chemistry was used to etch TaN and buffered oxide etch (BOE) was used to etch the SiO_2 layer. The process flow, a schematic cross-section of a stacked device, and a scanning electron microscopy (SEM) top-view image of similar devices are shown in Fig. 1. Current-voltage (*I-V*) characteristics were measured using an Agilent B1500A semiconductor device analyzer in vacuum ambient ($<1 \times 10^{-4}$ mbar). To characterize resistive switching, critical switching parameters were extracted for all samples—"Set Current/Reset Current (I_{set})/(I_{reset})" and "Set Voltage/Reset Voltage (V_{set})/(V_{reset})" are defined as the values of current and voltage measured at the initiation of resistance switching transitions between High Resistivity State (HRS) and Low Resistivity State (LRS). The definitions of "LRS Current"/"HRS Current" are the measured currents at 0.2 V bias for the LRS/HRS.

Figs. 2(a) and 2(b) show *I-V* characteristics of 30 switching cycles for samples in vacuum and pure N_2 ambient, respectively. Voltage was applied to the top electrode with bottom electrode at ground. The compliance current limit was set to 1 mA during each 4 V forward/reverse sweep used to program the device to the LRS. Unipolar switching is observed for both ambient conditions. By sweeping the voltage to 8 V, the current begins to decrease at V_{reset} and the device is programmed into a HRS. During the subsequent 4 V forward/reverse sweep, the current increases suddenly at V_{set} and sets the device to a LRS. The HRS/LRS resistance ratios for both are at least $\sim 10^2$ at 0.2 V, which satisfies sensing requirements.[9] Before switching cycle measurements, a one-

a)Author to whom correspondence should be addressed. Electronic mail: yfchang@utexas.edu.

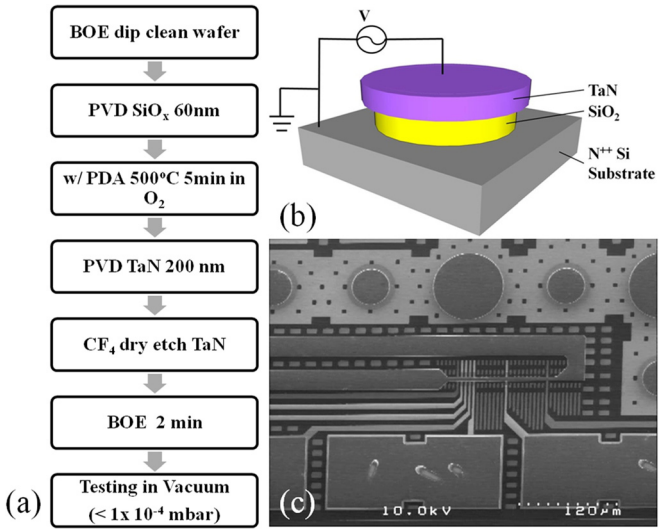

FIG. 1. (a) Process flow, (b) schematic cross-section of TaN/SiO_2/n^{++} Si-substrate structure, and (c) test structure layout.

time electroforming process is performed, where leakage current fluctuations are observed with increasing bias, as shown in the insets of Figs. 2(a) and 2(b). The required forming voltage to achieve current fluctuations of about 1 μA is larger for the sample in N_2 ambient (20 V) than for the sample in vacuum (8 V). The electroforming process is completed during the backward voltage sweep from forming voltage to 0 V, resulting in a LRS. In these devices, the reset voltage is always larger than the set voltage, which is unique as compared to other material systems.[10] The reset voltage is possibly larger than set voltage due to series resistance or external parasitic resistance during the measurement. Metal filament formation, for example, a Ta filament resulting from metal atoms diffusing into the SiO_x layer, can be ruled-out in this case since the *I-V* response maintains the characteristic response for SiO_x materials where $|V_{set}| < |V_{reset}|$.

The average values of key operating parameters for 30 resistive switching cycles are shown in Fig. 3 as a function of N_2 pressure. Fig. 3(a) shows that the set and reset power (voltage × current) have little dependence on N_2 pressure, illustrating that reversible switching is not affected by N_2 exposure and devices operate without degradation as comparison to an oxygen-containing ambient (as will be shown later). Both LRS and HRS currents increase with N_2 pressure when the devices are operated for several switching cycles at each N_2 pressure, as shown by the open symbols in Fig. 3(b). However, when devices are first set ON or OFF in vacuum at 10^{-4} Torr, and then simply read at 0.2 V without performing any switching cycles (a "non-destructive read" operation), the measured current is stable across all N_2 pressures (filled symbols in Fig. 3(b)). As compared to devices tested with the non-destructive read, the current in actively-switched ON- and OFF-state devices increased by 13X and 160X, respectively. To further characterize and confirm the switching-induced current increases in N_2 ambient, *I-V* data from 0 to 2 V were fit to the Frenkel-Poole characteristic, $I_{pf} = G \times \exp(\beta V^{-1/2})$, and charge transport parameters G and β were extracted. As shown in the Fig. 3(a) inset, the apparent relative permittivity, calculated from the β parameter,[11] increases substantially for both ON- and OFF-state devices. Based on our previous current fitting results and normalized conductance method,[7,12] the current transport behavior from 0 to 2 V for both LRS and HRS can be accurately fit to Frenkel-Poole emission, where the apparent relative permittivity values of LRS and HRS can be controlled using compliance current and reset voltage.[12] Furthermore, the apparent relative permittivity of LRS and HRS both increase with N_2 pressure, suggesting that the dielectric properties near the conductive filament are changed and tend to increase the apparent polarization as compared to operation in vacuum (Fig. 3(a) inset). Syu *et al.* have suggested that a N-doped switching layer may help control oxygen vacancy defects and stabilize switching performance due to nitrogen having high electronegativity when introduced into SiO_x-based materials.[13] Localized Joule heat is often considered to drive the reset process in filamentary devices,[14] suggesting that, as N_2 pressure is increased, more nitrogen may incorporate into the active switching region during repeated switching cycles as the result of a Joule heat-assisted process, essentially resulting in a N-doped switching layer.

In contrast to a N_2 ambient, a 20% O_2-N_2 mix limits the resistive switching range to ≤1 Torr, with device functionality becoming severely degraded at 10 Torr, as shown in Fig. 4(a). Interestingly, reversible switching can be re-established by performing a sweep from 0 to 8 V in vacuum, where resistive switching recovers to initial vacuum conditions (see inset of Fig. 4(a)). The statistical distribution of switching voltage as a function of 20% O_2-N_2 pressure is summarized in Fig. 4(b). Two operating modes are observed: (1) for pressures ≤1 Torr, resistive switching is not degraded and follows normal operating characteristics; and (2) at pressures at or above 10 Torr, resistive switching fails where V_{set} becomes <1 V and V_{reset} increases to >7 V. Our working

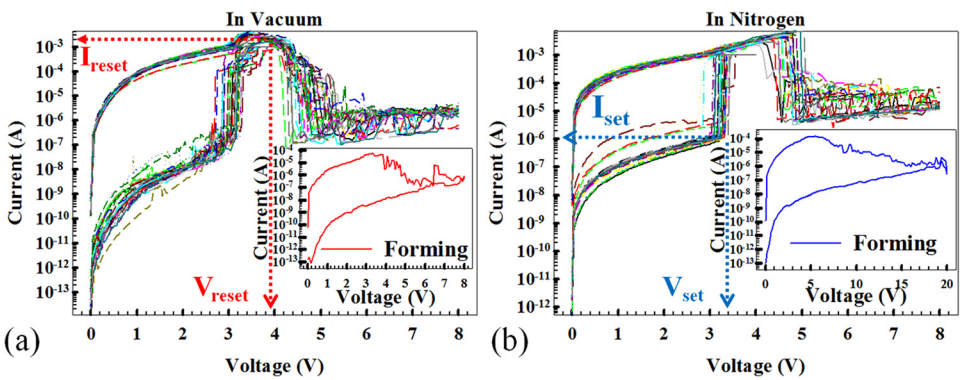

FIG. 2. The resistive switching behaviors and forming process (insets) in (a) vacuum and (b) N_2 ambient.

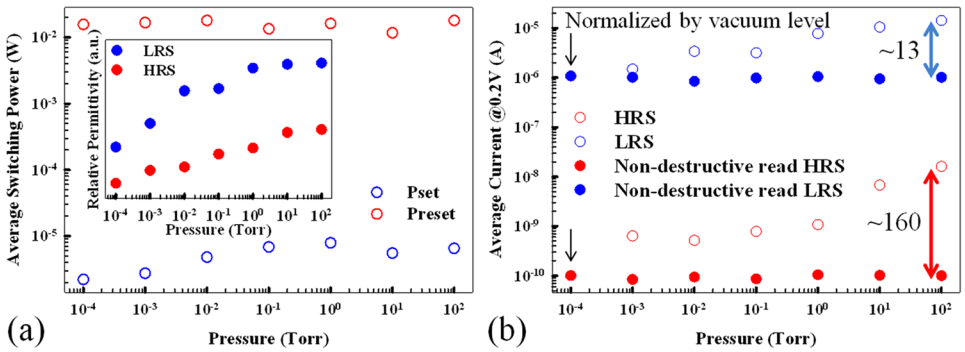

FIG. 3. (a) Average of switching powers, relative permittivity values for LRS and HRS by Frenkel-Poole fitting (inset) and (b) LRS and HRS as a function of N_2 pressure.

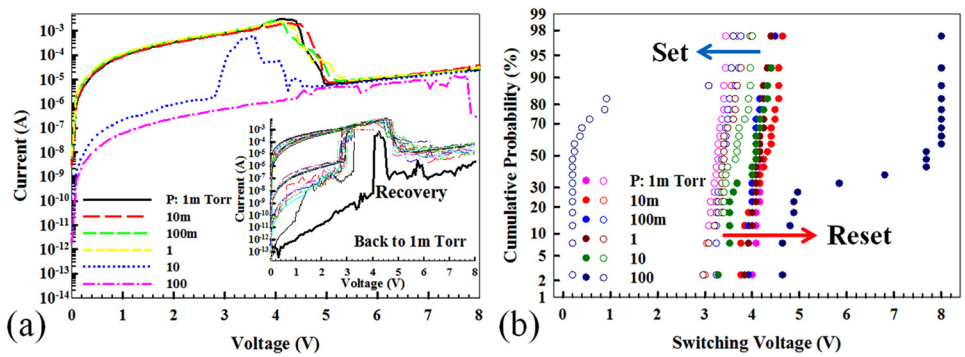

FIG. 4. (a) Average current for 20 set/reset cycles for different 20% O_2-N_2 pressures and recovery process in vacuum (inset). (b) Cumulative probability of switching voltage as function of 20% O_2-N_2 pressure.

hypothesis to explain these results is that the defects responsible for resistive switching (and current transport) are hydrogen-passivated in both the LRS (H-bridge) and HRS (H-doublet), thus protecting them from oxidation when biased up to 2 V in 1 atm of air;[15] however, when bias is increased above ~2.5 V, a switching event occurs and hydrogen passivation is temporarily lost, thereby allowing ambient O_2 to react with the defect and disable switching. Figs. 5(a) and 5(b) show the cumulative distribution function (CDF) of set and reset voltages at 10 and 100 Torr for 20% O_2-N_2 ambient. By using the bi-modal Monte Carlo simulation (repeated random sampling) and weakest link approximation,[16,17] the oxygen-induced failure mode can be modeled for failure analysis. The weakest link approximation applies when multiple elements are in series where failure of the first element causes failure of the device, leading to $F_N(t) = 1 - (1 - F_1(t))^N$, where N is the number of elements in the series and $F_1(t)$ is the CDF for single elements. The failure percentage values for set and reset processes are found to be 0.146% and 0.3%, respectively, which indicates that, for the same ambient conditions, the failure mechanism may be dominate during the reset process (HRS) due to the larger percentage of the weak failure mode. In other words, the effect of oxidation during defect-level transformations, especially when forming the H-doublet, severely suppresses resistive switching behavior. The simulation not only characterizes the failure mode information in detail but also provides additional insights into the critical oxygen content levels necessary for development of a possible oxygen sensor and the packaging requirements for oxygen detection when using SiO_x-based resistive switching devices.

In conclusion, ambient gas effects on resistive switching behaviors in the simple TaN/SiO_2/n^{++} Si-substrate structure were investigated. Electroforming voltage in N_2 ambient is larger than in vacuum but no degradation of resistive switching is observed. Possible N-incorporated into the active switching region by Joule heating may result in an increase of current at 0.2 V. Moreover, the oxygen-induced switching failure mode is observed in detail by controlling the pressure of the nitrogen-oxygen mix. It is found that exposure to ≥10 Torr 20% O_2-N_2 disables resistive switching, but normal switching behavior and can be recovered by applying a voltage sweep in vacuum. The statistical distribution of switching behaviors and failure modes were investigated using bi-modal Monte Carlo simulations, which establishes the oxygen detection levels for oxygen sensor development

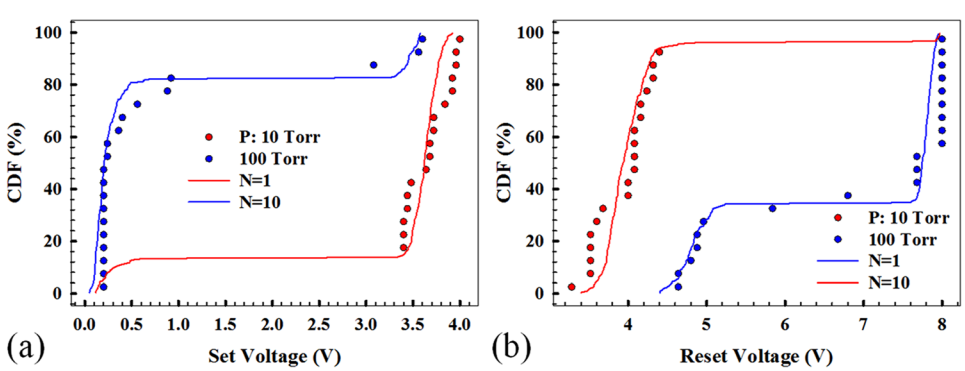

FIG. 5. Initiation of resistive switching failures above 10 Torr of 20% O_2-N_2 mixture showing the cumulative distribution function (CDF) using bi-modal Monte Carlo simulation fitting for (a) set and (b) reset voltage.

and the packaging requirements for SiO_x-based ReRAM for use in future applications.

This work was partially supported by PrivaTran LLC under Small Business Innovation Research Contract No. N66001-11-C-5212.

[1]Y. Y. Chen, R. Degraeve, S. Clima, B. Govoreanu, L. Goux, A. Fantini, G. S. Kar, G. Pourtois, G. Groeseneken, D. J. Wouters, and M. Jurczak, Tech. Dig. - Int. Electron Devices Meet. **2012**, 482.
[2]Y. S. Chen, H. Y. Lee, P. S. Chen, C. H. Tsai, P. Y. Gu, T. Y. Wu, K. H. Tsai, S. S. Sheu, W. P. Lin, C. H. Lin, P. F. Chiu, W. S. Chen, F. T. Chen, C. Lien, and M.-J. Tsai, Tech. Dig. - Int. Electron Devices Meet. **2011**, 717.
[3]S. Yu, B. Gao, Z. Fang, H. Yu, J. Kang, and H.-S. Philip Wong, Tech. Dig. - Int. Electron Devices Meet. **2012**, 239.
[4]Y. B. Kim, S. R. Lee, D. Lee, C. B. Lee, M. Chang, J. H. Hur, M.-J. Lee, G.-S. Park, C. J. Kim, U.-I. Chung, I.-K. Yoo, and K. Kim, Tech. Dig. - VLSI Technology **2011**, 52.
[5]J. Yao, Z. Sun, L. Zhong, D. Natelson, and J. M. Tour, Nano Lett. **10**, 4105 (2010).
[6]A. Mehonic, S. Cueff, M. Wojdak, S. Hudziak, C. Labbé, R. Rizk, and A. J. Kenyon, Nanotechnology **23**, 455201 (2012).
[7]Y. F. Chang, P. Y. Chen, B. Fowler, Y. T. Chen, F. Xue, Y. Wang, F. Zhou, and J. C. Lee, J. Appl. Phys. **112**, 123702 (2012).
[8]Y. F. Chang, P. Y. Chen, Y. T. Chen, F. Xue, Y. Wang, F. Zhou, B. Fowler, and J. C. Lee, Appl. Phys. Lett. **101**, 052111 (2012).
[9]C. J. Chevallier, H. S. Chang, S. F. Lim, S. R. Namala, M. Matsuoka, B. L. Bateman, and D. Rinerson, Dig. Tech. - Solid-State Circuits Conference (ISSCC) **2010**, 260.
[10]I. H. Inoue, S. Yasuda, H. Akinaga, and H. Takagi, Phys. Rev. B. **77**, 035105 (2008).
[11]Y. F. Chang, T. C. Chang, and C. Y. Chang, J. Appl. Phys. **110**, 053703 (2011).
[12]Y. F. Chang, P. Y. Chen, Y. T. Chen, F. Xue, Y. Wang, F. Zhou, B. Fowler, and J. C. Lee, Dig. Tech. - VLSI Technology, Systems and Applications **2013**, 42.
[13]Y. E. Syu, T. C. Chang, C. T. Tsai, G. W. Chang, T. M. Tsai, K. C. Chang, Y. H. Tai, M. J. Tsai, and S. M. Sze, Electrochem. Solid-State Lett. **14**, H419 (2011).
[14]U. Russo, D. Ielmini, C. Cagli, and A. L. Lacaita, IEEE Trans. Electron Devices **56**, 193 (2009).
[15]Y. T. Chen, B. Fowler, Y. Wang, F. Xue, F. Zhou, Y. F. Chang, P. Y. Chen, and J. C. Lee, IEEE Electron Device Lett. **33**, 1702 (2012).
[16]M. Ohring, *Reliability and Failure of Electronic Materials and Devices* (Academic Press, San Diego, 1998).
[17]P. A. Tobias and D. Trindade, *Applied Reliability* (CRC Press, New York, 1986).